

**This is the accepted manuscript version of the contribution published as:**

Laloo, A.E., Wei, J., Wang, D., Narayanasamy, S., Vanwonterghem, I., Waite, D., Steen, J., Kaysen, A., **Heintz-Buschart, A.**, Wang, Q., Schulz, B., Nouwens, A., Wilmes, P., Hugenholtz, P., Yuan, Z., Bond, P.L. (2018):

Mechanisms of persistence of the ammonia-oxidizing bacteria *Nitrosomonas* to the biocide free nitrous acid

*Environ. Sci. Technol.* **52** (9), 5386 - 5397

**The publisher's version is available at:**

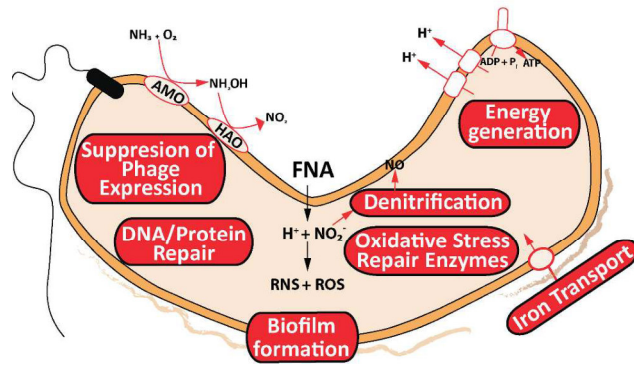
<http://dx.doi.org/10.1021/acs.est.7b04273>





24

### Abstract Art



25

26

27

28

29

30

31

32

33

34

35

36

37

38

39

40

41

42

43

44

45

46

47

48 **ABSTRACT**

49 Free Nitrous Acid (FNA) exerts a broad range of antimicrobial effects on bacteria  
50 although susceptibility varies considerably amongst microorganisms. Among nitrifiers found  
51 in activated sludge of wastewater treatment processes (WWTP), nitrite oxidising bacteria  
52 (NOB) are more susceptible to FNA compared to ammonia oxidising bacteria (AOB). This  
53 selective inhibition of NOB over AOB in WWTP bypasses nitrate production and improves  
54 the efficiency and costs of the nitrogen removal process in both the activated sludge and  
55 anaerobic ammonium oxidation (Anammox) system. However, the molecular mechanisms  
56 governing this atypical tolerance of AOB to FNA have yet to be understood. Herein we  
57 investigate the varying effects of the antimicrobial FNA on activated sludge containing AOB  
58 and NOB using an integrated metagenomics and label free quantitative sequential windowed  
59 acquisition of all theoretical fragment ion mass spectra (SWATH-MS) metaproteomic  
60 approach. The *Nitrosomonas* genus of AOB on exposure to FNA maintains internal  
61 homeostasis by upregulating a number of known oxidative stress enzymes such as pteridine  
62 reductase and dihydrolipoyl dehydrogenase. Denitrifying enzymes were upregulated on  
63 exposure to FNA suggesting the detoxification of nitrite to nitric oxide. Interestingly proteins  
64 involved in stress response mechanisms such as DNA and protein repair enzymes, phage  
65 prevention proteins as well as iron transport proteins were upregulated on exposure to FNA.  
66 Interestingly enzymes involved in energy generation were upregulated on exposure to FNA.  
67 The total proteins specifically derived from the NOB genus *Nitrobacter* was low and as such  
68 did not allow for the elucidation of the response mechanism to FNA exposure. These  
69 findings give us an understanding of the adaptive mechanisms of tolerance within the AOB  
70 *Nitrosomonas* to the biocidal agent FNA.

71

72

## 73 1. INTRODUCTION:

74

75 Studies on bacteria have shown that the protonated form of nitrite i.e.  $\text{HNO}_2$  also  
76 known as free nitrous acid (FNA), is a strong biocide [1]. Additionally, FNA was seen to  
77 have broad bacteriocidal and biocidal effects on an array of microorganisms, which have led  
78 to its use in a range of applications for wastewater treatment processes (WWTP). This  
79 includes the control of microbial induced sewer corrosion; the enhanced biodegradability of  
80 microbes in activated sludge to achieving reduced  $\text{N}_2\text{O}$  production in the activated sludge  
81 process [2-8]. It has been hypothesised that once inside the cell, FNA dissociates to form  
82 various reactive nitrogen species (RNS) and reactive oxygen species (ROS) speculated to  
83 enhance the toxicity of FNA, but the chemistry of this reaction is not well characterised [9].  
84 These reactive species can cause direct oxidative damage to cellular proteins, cell membrane  
85 and cell wall components as well as nucleic acids. It is hypothesised that FNA can act as a  
86 protonophore by collapsing the proton membrane potential and thereby inhibiting ATP  
87 production [10]. Further application of FNA for control of microbial growth and activity  
88 would benefit from improved understanding of how it causes toxicity to various  
89 microorganisms.

90

91 Transcriptomic based investigations have been conducted on *Pseudomonas*  
92 *aeruginosa* (PAO1) and *Desulfovibrio vulgaris* (Hildenborough) to determine the toxic  
93 mechanisms of FNA. At 0.1 mg/L FNA-N caused inhibition of cellular respiration that led to  
94 PAO1 re-routing its carbon metabolic pathway from the tricarboxylic acid (TCA) cycle to the  
95 pyruvate fermentation pathway. Inhibition of protein synthesis and inactivation of ribosome  
96 components was also evident [5]. Studies on PAO1 showed that FNA at 5.0 mg/L FNA-N  
97 caused cell death [11]. For the bacterium *D. vulgaris*, FNA caused increased expression of

98 genes coding for oxidative stress enzymes indicating that FNA caused oxidative stress as well  
99 as decreased anaerobic respiration and a shut down of protein synthesis[4].

100

101 In wastewater treatment processes (WWTP), the removal of nitrogen is carried out via  
102 the use of the activated sludge process. This is achieved by the actions of nitrifying and  
103 denitrifying bacteria in a multi-step process. Ammonium is converted to nitrite, by the  
104 ammonia-oxidising bacteria (AOB), and then converted to nitrate by the nitrite-oxidising  
105 bacteria (NOB). Denitrifying bacteria consequently reduces nitrite and nitrate to nitrogen gas  
106 [12-14]. The most commonly found nitrifying bacteria in activated sludge belong to the  
107 *Nitrosomonas* genus for the AOB and the *Nitrobacter* and *Nitrospira* genera for the NOB  
108 [15]. Interestingly, studies on activated sludge systems show that NOB species are more  
109 sensitive to FNA than AOB [10, 16, 17]. FNA concentrations of greater than 1.5 mg/L FNA-  
110 N are found to selectively inhibit the NOB population [16]. In a recent study the growth of  
111 NOB was selectively inhibited whereas the AOB population remained high when the sludge  
112 was treated with FNA at 1.8 mg/L FNA-N [15]. Fortuitously, this phenomenon could benefit  
113 nitrogen removal in WWTP as the suppression of NOB results in ‘partial nitrification’ where  
114 nitrite is formed instead of nitrate in both conventional nitrogen removal using activated  
115 sludge system and the anaerobic ammonium oxidation (Anammox) [15]. This can lead to  
116 high economic and operational benefits for WWTP due to the decreased oxygen demand for  
117 nitrification, less organic carbon required for denitrification and potentially reduced N<sub>2</sub>O  
118 emissions [6].

119

120 Despite the range of applications of FNA in WWTP, there is limited understanding of  
121 the increased tolerance of AOB over NOB to the biocide. NOB, in general have two  
122 additional pathways to remove toxic nitrite build up compared to AOB (Figure S1). AOB and

123 NOB both have the nitrite detoxifying gene nitrite reductase (*nirK*) that converts nitrite to  
124 nitric oxide (NO) [18]. The nitrite reductase (*nirBD*) and nitrite oxidoreductase (*norA/B*)  
125 genes, present exclusively in NOB convert nitrite to ammonia and nitrate respectively thereby  
126 detoxifying toxic nitrite. The limited numbers of detoxifying pathways in AOB is contrary to  
127 its observed tolerance. To date there is no clear understanding of the underlying mechanisms  
128 that govern this tolerance to FNA.

129

130         Studies investigating the global responses of AOB to various stress conditions are  
131 sparse and have been limited to responses to iron stress, toxic zinc exposure, oxidative stress  
132 induced by hydrogen peroxide and starvation [19-22]. In this study we reveal the reasons for  
133 FNA tolerance in AOB compared to NOB using a combined metagenomic and a quantitative  
134 sequential windowed acquisition of all theoretical fragment ion mass spectra (SWATH-MS)  
135 metaproteomic approach. SWATH-MS is a label free proteomics approach that allows for the  
136 unbiased, reproducible quantification of essentially any protein of interest without the use of  
137 expensive labelling approaches [23]. Additionally SWATH-MS requires low amounts of  
138 proteins (1 µg) for analysis along with a 5 µg aliquot of pooled samples for the creation of a  
139 spectral library using information dependent acquisition (IDA) [23]. Of the reports on  
140 microbial metaproteomics, to our knowledge this study describes the first use SWATH-MS  
141 on an environmental microbiome sample.

142

## 143 **2. MATERIALS AND METHODS**

### 144 2.1. Reactor set up, side stream treatments and sampling:

145         An 11 L sequencing batch reactor (SBR) originally seeded with activated sludge from  
146 a domestic wastewater treatment plant in Brisbane, Australia was operated in a temperature  
147 controlled room (22±1 °C) supplied with an ammonium based synthetic feed sans organic



148 carbon for the selection of nitrifying bacteria. The synthetic wastewater composition per liter  
149 was: 0.2949 g of  $\text{NH}_4\text{HCO}_3$  (57 mg  $\text{NH}_4^+\text{-N}$ ), 0.33 g  $\text{NaHCO}_3$ , 0.184 g of  $\text{NaCl}$ , 0.072 g of  
150  $\text{NaH}_2\text{PO}_4\cdot\text{H}_2\text{O}$ , 0.035 g  $\text{MgSO}_4\cdot 7\text{H}_2\text{O}$ , 0.029 g  $\text{KCl}$  and 0.3 mL of a trace element stock  
151 solution prepared as previously described [24]. The reactor was operated with four cycles  
152 daily (6 hours each), which consisted of a 90 min aerobic feed period wherein 5L of synthetic  
153 wastewater was pumped into the reactor, a 210 min aerobic mixing period, a 50 min settling  
154 stage and a 10 min decanting period. No sludge was wasted during the study. During aeration  
155 periods, a dissolved oxygen (DO) concentration of 2.5-3.0 mg/L and a pH of 7.5 were  
156 maintained in the reactor using programmed logic controllers. The hydraulic retention time  
157 (HRT) of the reactor was 13.2 hours. At different SBR operational stages, a side stream  
158 treatment of FNA was applied to the sludge that was removed and then returned to the reactor  
159 (Figure 1(A)). In Stage 1 of the SBR operation, there was no FNA side stream treatment. In  
160 Stage 2, 2750 ml (25%) of the mixed liquor was withdrawn every day (second daily cycle)  
161 from the main SBR at the end of the aerobic stage (before settling) and the sludge was  
162 thickened to 130 ml. The sludge was then treated for 24 hours with an initial concentration of  
163 3.64 mg/L FNA-N (Stage 2) while maintaining a pH of 6.0 in a side stream FNA treatment  
164 reactor using a programmed logic controller. Following FNA treatment, the sludge was then  
165 returned to the main SBR. At the end of the second daily cycle, the amount of treated  
166 wastewater decanted was altered so that the 13.2 h HRT was maintained. Similarly, in Stage  
167 3 the same sludge treatment was carried out every day with a changed side stream FNA  
168 treatment of 1.82 mg/L FNA-N. The nitrogen species of the side stream reactor were  
169 measured at 0 and 24 hours following treatment.

170

171 For the metagenomic investigation, samples of mixed liquor were collected at the end  
172 of each stage of operation from the main reactor. The samples once collected were

173 centrifuged at 14,000 x g for 2 mins (4 °C) and the supernatants removed. The remaining  
174 pellets were snap frozen in liquid nitrogen (-196 °C) to eliminate enzymatic activity and then  
175 stored at -80 °C until DNA extractions were performed. For the metaproteomic studies,  
176 samples were collected at the end of Stage 3, from where the thickened sludge (130 ml) was  
177 equally distributed to an FNA treatment reactor at 1.82 mg/L FNA-N and a control reactor  
178 without FNA treatment i.e. 0 mg/L FNA-N. Triplicate samples for metaproteomics were  
179 taken from both side stream reactors at the treatment times of 0 min, 20 min, 2 hours, 12  
180 hours and 24 hours for 3 consecutive days. Following centrifugation, supernatant was  
181 removed and pellets were snap frozen in liquid nitrogen and stored at -80 °C until protein  
182 extraction was carried out.

183

#### 184 2.2. Analytical methods and DNA extraction:

185 The ammonium, nitrite and nitrate concentrations in the SBR effluent were measured  
186 2-4 times every week using a Lachat QuikChem8000 Flow Injection Analyzer (Lachat  
187 Instrument, Milwaukee, Wisconsin, USA). Microbial DNA was extracted from sludge  
188 samples for metagenomics using the PowerSoil® DNA isolation Kit (MO BIO Laboratories)  
189 as per the manufacturer's instructions. Metagenomic DNA was sequenced using the Illumina  
190 NextSeq 500 platform using the Nextera library protocol (Illumina) at the Australian Centre  
191 for Ecogenomics, University of Queensland.

192

#### 193 2.3. Metagenomic assembly and analyses:

194 Raw DNA sequences were added to the Metagenomics Rapid Annotation (MG-  
195 RAST) server (v4) for rapid annotation and the determination of microbial community  
196 composition at the three different stages of the reactor operation. The sequence datasets for  
197 the stages 1, 2 and 3 were loaded into MG-RAST with identifications of mgm4688234.3,

198 mgm4688240.3 and mgm4688237.3 respectively [25]. The raw Illumina sequence reads were  
199 also processed using two different bioinformatic pipelines to create a robust and tailored  
200 metagenome database. Briefly, in the first pipeline (Pipeline 1), adaptors of the forward and  
201 reverse reads were clipped and quality trimmed with trimmomatic using a minimum quality  
202 score of 3 for leading and trailing bases, along with a minimum average quality score for 4 bp  
203 as 15 limiting the minimum required length to 50bp [26]. Additionally microbial community  
204 analysis was carried out using the GraftM tool wherein reads were parsed through GraftM to  
205 identify those containing 16S reads using the May, 2015 Greengenes database 97% OTUs  
206 (operational taxonomic units) as a reference with default parameters [27]. The quality  
207 controlled reads were then merged with BBmerge [28]. The quality controlled paired reads  
208 were assembled using CLC Genomics Cell assembler v8.0. The assembled contigs were then  
209 binned using GroopM and Metabat [29, 30]. In the second bioinformatic pipeline (Pipeline 2)  
210 the raw reads were processed using an automated pipeline called IMP (Integrated Meta-omic  
211 Pipeline) that involved iterative co-assembly and mapping [31]. The metagenome bins were  
212 generated through this pipeline using a VizBin-based workflow [32, 33]. The quality of the  
213 bins generated from both these bioinformatic pipelines were then estimated using CheckM.  
214 Taxonomies of the bins were inferred using the genome taxonomy database (GTDB) [34].  
215 Nitrifying population genome bins with greater than 75% completeness and contamination  
216 less than 10 % were annotated using Prokka and concatenated to create a custom tailored  
217 database for metaproteomics [35, 36].

218

#### 219 2.4. Protein extraction and digestion:

220 Protein extraction was carried out on all triplicate samples collected from the side  
221 stream treatment reactor under 1.82 mg/L FNA-N and a 0 mg/L FNA-N as a control. A 10ml  
222 protein extraction buffer was prepared using 10 ml of B-PER Bacterial Protein Extraction

223 Reagent mix (Thermo Fisher Scientific), 7.7 mg of dithiothreitol and 1 tablet of Complete  
224 mini EDTA-free Protease Inhibitor Cocktail (Roche). 1 ml of this buffer was added to each  
225 thawed sludge pellet (Section 2.1) for extraction and left at room temperature for 30 minutes  
226 with periodic vortexing to solubilise the protein. The cell debris was removed after  
227 centrifugation at 15,000 g for 15 mins following which the protein supernatant was incubated  
228 overnight with 10% Trichloroacetic acid (TCA) at 4 °C. The protein was recovered by  
229 centrifugation at 18,000 g for 15 mins following which the pellets were washed twice with  
230 cold acetone and subsequently dried at room temperature. Once dried the pellets were re-  
231 suspended in 100 µl of buffer containing 2 M thiourea, 7 M urea and 100 mM ammonium  
232 bicarbonate. Protein quantification was carried out through the 2-D Quant Kit (GE  
233 Healthcare). Subsequently, reduction of proteins was carried out with 5 mM dithiothreitol  
234 for 30 mins at 56 °C. Alkylation of the protein was carried out by incubation in the dark for  
235 30 mins at room temperature with 25 mM iodoacetamide (Sigma-Aldrich). Additional 50  
236 mM dithiothreitol was added to quench the alkylation reaction once the incubation was  
237 complete. Samples were diluted with 50 mM ammonium bicarbonate to reduce the urea  
238 concentration to 2 M. Digestion with 1:50 trypsin:protein ratio was performed at 37 °C for 4  
239 hours. Following that a second digestion was performed with a 1:25 trypsin:protein ratio at  
240 37 °C overnight [37]. Peptides were further concentrated and purified using the C-18  
241 ZipTip® Pipette Tips (Merck Millipore) using 5% acetonitrile/0.1% trifluoroacetic acid for  
242 washing and then elution with 80% acetonitrile/0.1% trifluoroacetic acid. The samples were  
243 dried using a Speed-Vac to remove acetonitrile and peptides were re-suspended in 0.1%  
244 formic acid into vials used for mass spectrometry (Agilent Technologies) [38].

245

246 2.5. Metaproteomic analysis:

247           Following purification, 1  $\mu\text{g}$  of digested protein was used for SWATH acquisitions  
248 and 5  $\mu\text{g}$  aliquots of pooled samples were used to create a spectral library using information  
249 dependent acquisition (IDA) mode. Peptides were directly analysed on a LC-ESI-MS/MS  
250 with a Prominence nanoLC system (Shimadzu) and a Triple-ToF 5600 instrument (ABSciex)  
251 equipped with a Nanospray III interface as previously described [39]. Mass spectrometry  
252 (MS) data of pooled IDA samples was searched using ProteinPilot™ software (ABSciex,  
253 Forster City CA) against a custom tailored database containing the population genome bins of  
254 nitrifiers generated from both the metagenomic pipeline analysis (Table 1) and the genomes  
255 of known nitrifiers downloaded publically from Uniprot Swiss-Prot database (June 2016  
256 release). The search settings included enzyme digestion set to trypsin, cysteine alkylation set  
257 to iodoacetamide, and global false discovery rate (FDR) set at 1%. The quantified proteome  
258 SWATH files were generated using the PeakView with 5 peptides per protein and 3  
259 transitions per peptide. The MSstats package in R was used for statistical analysis of the  
260 spectral information and the p-value stringency was set to  $\leq 0.05$  across triplicate samples  
261 [40]. To determine the  $\log_2(\text{FC})$  ( $\log_2$  Fold change) of proteins we compared the 0 minutes  
262 time point to the other time points wherein samples were collected i.e. 20 minutes, 2 hours,  
263 12 hours and 24 hours at the two FNA concentrations using the ‘groupComparison’ function  
264 of MStats. The sequences, molecular functions and biological processes of the proteins were  
265 queried and verified against the curated UNIPROT and NCBI databases [41]. Additional  
266 statistical analysis was carried out at each sample time-point between the control and the  
267 FNA treated sample to verify the statistical significance of  $\log_2(\text{FC})$  protein expression.

268

### 269 **3. RESULTS AND DISCUSSION:**

#### 270 3.1. Reactor performance:

271 The SBR was operated for nitrification activity in three main stages. In Stage 1 there  
272 was no side stream treatment of the activated sludge and near complete conversion of  
273 ammonium to nitrate occurred ( $97.0 \pm 0.7\%$ ; Figure 1A). This was due to the high activity of  
274 both AOB and NOB (Figure 1B). During Stage 2, when part of the sludge was treated at 3.64  
275 mg N/L FNA-N in the side stream treatment reactor, the levels of nitrate in the effluent  
276 decreased sharply (Figure 1B), indicating that the NOB population was severely inhibited.  
277 This coincided with high levels of nitrite in the effluent, manifested by the activity of AOB at  
278 the high FNA treatment. An increase in ammonium was detected in the effluent after day 55  
279 of operation, indicating there was some inhibition of AOB activity by the high FNA sludge  
280 treatment. At this point the side stream FNA treatment was terminated for a 10-day period to  
281 recover AOB activity. In Stage 3 a side stream treatment of FNA at 1.82 mg N/L was applied  
282 to the SBR sludge for 24 hours at a pH of 6.0. The measured nitrogen species, including VSS  
283 and other parameters including the activity of the AOB and NOB populations at the end of  
284 both stages 1 and 3 have been summarized in Table S1. Additionally nitrogen species  
285 measurements of the side stream FNA reactor at stage 3 is represented in Table S2 During  
286 this treatment ammonium in the mainstream SBR reactor was nearly completely converted to  
287 a mixture of nitrite ( $58.5 \pm 0.3\%$  of the total effluent nitrogen) and nitrate ( $40.2 \pm 0.7\%$  of the  
288 total effluent nitrogen) (Figure 1B). Thus, at this level of treatment AOB were active and  
289 there was some activity of NOB. The results of the SBR operation are in agreement with  
290 previous studies showing that AOB are less sensitive to FNA toxicity in comparison to NOB  
291 [6, 15]. Consequently, FNA could be used to effectively control the NOB and AOB  
292 population and thereby the levels of nitrogen species produced, which can practically be  
293 beneficial to achieve the more economically favorable partial nitrification compared to the  
294 conventional nitrification and denitrification of WWTP. This control could also allow for the

295 effluent to be directly used for the treatment of a low organic carbon stream operating for  
296 nitrogen removal in a two-stage anaerobic ammonia oxidation (ANAMOX) system [42].

297

298 (Position for Figure 1)

299

300 3.2. Microbial community composition of the reactor:

301 As expected the synthetic wastewater feed containing ammonium and no organic  
302 carbon provided an amiable environment for the growth of autotrophic nitrifiers [43].  
303 Microbial community composition generated from MG-RAST were extracted and  
304 represented as percentages (Figure 1C). Nitrifiers dominated the microbial community in the  
305 SBR, however, a variety of low abundance heterotrophic bacteria were also detected. Among  
306 the nitrifiers, the 3 genera of AOB in the reactor included *Nitrosomonas*, *Nitrospira*,  
307 *Nitrosococcus* and 3 genera of NOB detected included *Nitrobacter*, *Nitrospira* and  
308 *Nitrococcus* (Table S2). The dominant AOB genus *Nitrosomonas* represented 20.48%,  
309 11.92% and 21.94% of the microbial communities within the reactor operation Stages 1, 2  
310 and 3 respectively. It is worth noting the drop in the *Nitrosomonas* populations during Stage  
311 2, suggesting that the high FNA treatment caused killing of some of these more resilient  
312 nitrifiers. This is in agreement with the increase in ammonium detected in the effluent, at  
313 nearly 20 mg/L around day 55 of the SBR operation (Figure 1B). After the sludge FNA  
314 treatment was stopped, the activity of the AOB population recovered as can be seen on day  
315 71 of the SBR operation (Figure 1B). For NOB in the SBR, the dominant genus *Nitrobacter*  
316 constituted 1.56%, 2.95% and 3.18% of the microbial communities in Stages 1, 2 and 3  
317 respectively (Table S2). Additionally, relative abundance of the microorganisms in these  
318 Stages was determined by GraftM, and this showed similar results to those obtained through  
319 MG-RAST (Table S2(b)). The AOB family *Nitrosomonadaceae* represented 30.23 %, 8.33 %

320 and 35.26 % of Stage 1, 2 and 3 respectively. The NOB genus *Nitrobacter* represented 0.05  
321 %, 0.16 % and 0.06 % of the microbial community from Stage 1, 2 and 3 (Table S3). Despite  
322 relatively low proportions of the NOB community the NOB activity was high in Stage 1 as  
323 evidenced by the nitrate detected (Figure 1B).

324

### 325 3.3. Nitrifier genomes detected in the reactor

326 The population genome bins of nitrifiers generated using the 2 bioinformatic pipelines  
327 with completeness cut-off of greater than 75% and a contamination less than 10 were  
328 obtained from the SBR. They included the NOB genus *Nitrobacter* and the AOB genus  
329 *Nitrosomonas* as represented in Table 1. The genera of the detected population genome bins  
330 are in agreement with the dominant nitrifiers detected from the MG-RAST analysis (Figure  
331 1C). A custom sequence database was generated using the annotated population genomes of  
332 nitrifiers obtained from the SBR together with annotated genomes of publically available  
333 *Nitrobacter* and *Nitrosomonas* species [44]. This custom database was used to maximise the  
334 detection of proteins for our metaproteomic analyses.

335

336 (Position for Table 1)

337

### 338 3.4. Metaproteomic responses of nitrifiers to FNA:

339 The SBR operation towards the end of Stage 2 i.e. 3.64 mg/L FNA-N was  
340 characterized by fluctuations in the nitrogen species (Figure 1B). This suggests that the FNA  
341 concentration was high enough to even suppress growth of AOB. The metaproteomic  
342 investigation of nitrifiers was carried out at Stage 3 i.e. 1.82 mg/L FNA-N as the operation of  
343 the SBR reactor was stable as evidenced from the nitrogen species of the effluent (Figure  
344 1B). Metaproteomic investigation was also carried out on a control sample i.e. 0 mg/L FNA-



345 N to compare the responses to nitrifiers without FNA treatment. Using the ProteinPilot™  
346 software a total of 419 proteins were identified against the custom database at a global FDR  
347 of 1%. The SWATH files generated from the Peak View software were analysed using the R-  
348 package MSstats. A total of 359 proteins met the p-value stringency of  $\leq 0.05$  across  
349 triplicates of which 344 originated from the *Nitrosomonas* genera and 15 from the  
350 *Nitrobacter* genera (Figure S2). The quantitative SWATH-MS analysis on the *Nitrosomonas*  
351 genera showed changed expression of various proteins, which have been discussed below (for  
352 detailed description see Supplementary Table 1). The mass spectrometry data has been  
353 deposited to the ProteomeXchange Consortium via the PRIDE partner repository with the  
354 accession no: PXD007514 [45]. Additionally statistical analysis summarising the change in  
355 protein expression between the control (0 mg/L FNA-N) and 1.82 mg/L FNA-N (p-value  
356 stringency of  $\leq 0.05$  across triplicates) at 20 minutes, 2 hours, 12 hours and 24 hours were  
357 also investigated. The results of this analysis have been represented in Supplementary table 2.

358

### 359 3.4.1. Metaproteomic response

#### 360 3.4.1.1. *Nitrosomonas* genus

361 The change in the regulation and expression of proteins is likely due to the change in  
362 expression of the gene. As such changed protein expression levels reveal the responses of  
363 microorganism to a perturbed condition. In our study we compared the change in protein  
364 expression over time without FNA (control) treatment to the perturbed 1.82 mg/L FNA-N  
365 samples. The quantitative metaproteomic approach revealed the upregulation and  
366 downregulation of a number of cellular proteins by *Nitrosomonas* in response to the  
367 antimicrobial action of FNA. Functionally a majority of these proteins have not been well  
368 studied in bacterial systems, however they are expected to fulfil similar roles within bacteria.

369

370 *Oxidative stress enzymes:*

371 *Nitrosomonas* like other aerobic bacteria, experiences oxidative and nitrosative stress  
372 from a variety of sources in its natural environment. The few oxidative stress studies on AOB  
373 have been limited to catalase and superoxide dismutase (SOD) [22, 46, 47]. A number of  
374 proteins involved in oxidative stress were upregulated after a period of exposure to FNA.  
375 These included pteridine reductase and S-adenosylmethionine synthase (Figure 2(A)). The  
376 oxidative stress enzyme cytochrome *c*<sub>551</sub> peroxidase was however upregulated in both the  
377 control and perturbed condition (Figure 2(A)). Statistical analysis between the control and  
378 perturbed condition at 24 hours showed that cytochrome *c*<sub>551</sub> peroxidase (Ns76) was  
379 upregulated by 0.42 log<sub>2</sub>(FC) (Supplementary Table 2). An upregulation of these enzymes  
380 shows evidence that FNA induces oxidative damage on *Nitrosomonas*. This stress reaction is  
381 thought to primarily occur due to the presence of reactive oxygen and nitrogen species  
382 (ROS/RNS) [48]. The enzyme pteridine reductase is widespread in proteobacteria, and has  
383 been well studied in the protozoan parasite *Leishmania* where it is known to reduce the  
384 susceptibility of the protozoan to ROS and RNS [49]. A log<sub>2</sub>(FC) of S-adenosylmethionine  
385 synthase from 0.54 to 1.44 at 12 hours and 24 hours respectively on exposure to 1.82 mg/L  
386 FNA-N was seen (Supplementary Table 1). S-adenosylmethionine synthase is an enzyme  
387 known to produce S-adenosylmethionine, an important methyl donor for methylation of  
388 DNA, RNA, proteins and other macromolecules essential for normal gene regulation [50]. S-  
389 adenosylmethionine is known for preventing oxidative stress and has also been implicated in  
390 functioning as a neuroprotective agent in mice [51]. Furthermore, S-adenosylmethionine has  
391 been associated with attenuating oxidative stress in ethanol-LPS-Induced fibrotic rat models  
392 [52]. Increased abundance of cytochrome *c*<sub>551</sub> peroxidase was detected for several  
393 *Nitrosomonas* population bins in both the control and FNA exposed conditions (Figure 2(A)).  
394 Cytochrome *c*<sub>551</sub> peroxidase has known antioxidant activity that catalyses the reduction of

395 toxic H<sub>2</sub>O<sub>2</sub> [53]. Cytochrome *c* apart from being a part of the electron transport chain can also  
396 suppress ROS [54]. Previous studies have shown strong evidence in support of its protective  
397 function on deoxyribose against oxidative damage in vivo [55]. The antioxidant protein  
398 thioredoxin and its associated domain proteins were also upregulated on exposure to FNA  
399 [56]. Thioredoxin is a key protein involved in the oxidative stress response in plants [57].  
400 Thioredoxin, in mammalian endothelial cells has also been known to be involved in a  
401 regenerative machinery to regenerate proteins inactivated by oxidative stress [58].  
402 Additionally, thioredoxin in *Streptococcus pneumoniae* were also found to resist oxidative  
403 stress conditions [59]. Dihydrolipoyl dehydrogenase enzyme is known to be an active nitric  
404 oxide scavenger by reducing ubiquinone to ubiquinol, thus providing strong evidence for the  
405 action of RNS formed from FNA [60]. Peptide methionine sulfoxide reductase (msrA) is a  
406 repair enzyme that repairs protein inactivated by oxidation [61, 62]. The msrA derived from  
407 Ns85 was seen to be upregulated at 24 hours after exposure to 1.82 mg/L FNA-N. SOD is  
408 known to act as a strong antioxidant wherein it converts two molecules of superoxide to  
409 oxygen and hydrogen peroxide. Hydrogen peroxide is removed by catalase and peroxidase  
410 enzymes [63]. Whilst we did not detect the expression of catalase enzyme we did see a slight  
411 decrease in expression of the protein SOD (Ns76) over 24 hours after exposure to 1.82 mg/L  
412 FNA-N (Supplementary Table 1). However, according to the ProteinPilot analysis this SOD  
413 had high spectral coverage (66%) suggesting this is a highly abundant protein in the cell.  
414 Studies by Wood *et al.* (2001) describes the SOD as constitutively expressed [22]. This slight  
415 change in expression we detected supports the suggestion that SOD is constitutively  
416 expressed and that the *Nitrosomonas* has a high innate ability to deal with oxidative stress  
417 from SOD as well as from other proteins that are discussed here. Overall there is clear  
418 evidence showing that FNA mediates an oxidative stress response on *Nitrosomonas* possibly  
419 through ROS and RNS [64].

420

421 *Enzymes involved in nitrogen metabolism and energy conversion.*

422 Denitrifying enzymes are thought to protect AOB from the negative effects of nitrite  
423 [65]. An increased expression level of the denitrifying enzyme nitrite reductase in  
424 *Nitrosomonas* was detected during FNA treatment (Figure 2(B)). Nitrite reductase is known  
425 to reduce toxic nitrite to nitric oxide (NO), a free radical in a process known as nitrifier  
426 denitrification [66]. Interestingly nitrite reductase is thought to confer tolerance against nitrite  
427 as seen in a pure culture of *Nitrosomonas europaea* [67]. Oxygen sensitive hydroxylamine  
428 reductase, which catalyses the reduction of hydroxylamine to ammonia and water was  
429 upregulated in both the control and perturbed conditions [68]. However, at 1.82 mg/L FNA-  
430 N the protein was upregulated by 1.48 log<sub>2</sub>(FC) at 24 hours (Supplementary Table 2),  
431 signifying that perhaps the minor increase in the ammonia concentration in the FNA reactor  
432 could possibly be explained by the action of this enzyme (Table S2).

433

434 The key nitrifying and energy generation enzymes in AOB, ammonia monooxygenase  
435 (AMO) and hydroxylamine oxidoreductase (HAO) were detected in multiple *Nitrosomonas*  
436 genomes of the SBR sludge (Figure 2(B)). The detected increased abundance of these  
437 proteins on exposure to FNA is of interest as the side stream FNA treatment reactor has  
438 limited availability of ammonia, high concentration of nitrite and low availability of  
439 dissolved oxygen (Table S2). The stress induced by FNA and the need to maintain internal  
440 homeostasis causes the *Nitrosomonas* genera to use energy dependent mechanisms. This  
441 results in the upregulation of enzymes such as AMO and HAO, in anticipation of available  
442 ammonia for energy generation. This is in agreement with a previous study showing  
443 consistently high levels of AMO and HAO enzymes in *Nitrosomonas* for long periods  
444 (months) even in the absence of ammonia [69]. A previous study showed that nitrite inhibited

445 the AMO enzyme activity but did not investigate the expression levels of this enzyme [70].  
446 Of interest to note is the variation of protein expression of the same protein within different  
447 *Nitrosomonas* populations of the same genus (Figure 2(B)). A number of proteins involved in  
448 the energy generation pathways including ATP synthase subunits and cytochrome *c* oxidase  
449 subunits were seen to be upregulated on exposure to FNA (Figure 2(B)) [71]. The observed  
450 upregulation of these proteins in exposure to FNA strongly suggests that FNA initiates the  
451 generation of more ATP possibly used up in the energy dependent mechanisms of internal  
452 homeostasis.

453

454

455 (Position for Figure 2)

456

457 *DNA/Protein repair*

458 FNA has also been postulated to directly act on protein and DNA through ROS and  
459 RNS intermediates [72]. As such FNA exposure would result in the upregulation of a number  
460 of enzymes involved in DNA and protein repair [64]. Among the DNA repair enzymes,  
461 single stranded DNA-binding protein was upregulated on exposure to FNA (Figure S3(A)).  
462 This protein is known to be involved in DNA mismatch, recombinational damage repair  
463 mechanisms as well as SOS response [73]. The histone like DNA-binding protein HU-beta  
464 protein that is known to prevent denaturation of DNA by wrapping itself around it was  
465 upregulated on exposure to 1.82 mg/L FNA-N [74]. In contrast, the DNA helicase RecQ, a  
466 DNA repair enzyme in both human and bacteria was however observed to be downregulated  
467 with and without FNA exposure [75].

468

469 Expression of a number of proteins involved in protein repair mechanisms also  
470 changed on exposure to FNA. Protein-L-isoaspartate *O*-methyltransferase in humans is  
471 known to recognise damaged proteins and is involved in repairing them [76, 77]. Peptide  
472 methionine sulfoxide reductase (MsrA), an important repair enzyme for proteins that have  
473 been damaged on oxidation, again was upregulated, thus shedding evidence to the oxidative  
474 damage induced by FNA exposure [61, 62, 78]. The chaperone protein ClpB in bacteria is  
475 known to be part of the stress induced multi-chaperon system and it is known to help in the  
476 refolding of denatured stress-damaged protein [79]. This protein was however undetected in  
477 the control. Previous studies carried out on *Nitrosomonas europaea* showed that the response  
478 of the oxidation of chloroform increased the expression of ClpB, 6 to 10 fold in response to  
479 oxidation caused by chloroform [80]. The evidence of ClpB and MsrA being upregulated  
480 strongly supports the evidence that FNA causes oxidative damage to proteins. Other proteins  
481 found to be associated with protein repair include the 60 kDa and 10 kDa chaperonins. These  
482 chaperonins are essential for the folding of proteins in bacteria but little can be drawn from  
483 their expression in response to FNA [81].

484

485 *Other stress responses:*

486 Evidence from the metaproteomic analysis shows that FNA activated a number of  
487 other stress responses within the *Nitrosomonas* genus as evidenced by the change in protein  
488 expression as shown in Figure S3(B). The protein “AAA domain/putative AbiEii toxin/Type  
489 IV TA system” is an altruistic cell death system that is activated by phage infection thereby  
490 limiting viral replication [82]. This suggests that FNA caused the activation of the temperate  
491 phage and that *Nitrosomonas* suppresses the expression of this phage. Studies carried out in  
492 *Pseudomonas aeruginosa* on being exposed to nitric oxide (NO), a free radical that could  
493 possibly be formed from FNA showed that NO exposure caused bacteriophage genes to be

494 upregulated [83]. The modulator of FtsH protease HflK is known to govern the  
495 lysogenization frequency of phage lamda in the bacteria *E. coli* [84]. In our study there was a  
496 slight decrease in the expression of this protein. The bleomycin resistance protein, known to  
497 repair DNA breakage and lesions was upregulated on exposure to FNA (Figure S3(B)) [85,  
498 86].

499

500 Biofilm formation in the *Nitrosomonas* genus of AOB is not thoroughly understood  
501 but biofilm formation has been shown to be enhanced by the growth of other heterotrophic  
502 bacteria [87]. It is of interest to note that biofilm formation has been previously induced in  
503 *Nitrosomonas* on exposure to higher concentrations of the RNS/ROS nitric oxide [88]. Beta-  
504 lactamase hydrolase-like protein and alginate export proteins play an important role in the  
505 formation of biofilms [89, 90]. The protein alginate export is known to export alginate, a  
506 model extracellular polysaccharide (EPS) externally to aid in the formation of a protective  
507 biofilm. The expression of beta-lactamase hydrolase-like protein and alginate export protein  
508 increased after FNA exposure suggesting that *Nitrosomonas* is inducing growth of biofilm to  
509 protect itself from the biocidal action of FNA (Figure S3(B)). Alginate export expression was  
510 seen to change positively after exposure to FNA. On the other hand  
511 phosphomannomutase/phosphoglucomutase, a protein associated with the production of  
512 alginate and lipopolysaccharide (LPS) biosynthesis, was severely downregulated on exposure  
513 to FNA [91].

514

515 Of the detected proteases involved in proteolysis, the protease HtpX was the only one  
516 seen to be upregulated in the FNA treated sample. Protease HtpX, is a membrane bound  
517 metalloprotease that is known to be a stress-controlled protease possibly degrading damaged

518 oxidised proteins [64, 92]. This evidence lends further support to the fact that FNA causes  
519 oxidative damage to the proteins.

520

521 FNA exposure is seen to alter iron bioavailability within the cell through the RNS and  
522 ROS that are formed. A number of enzymes contain iron as a co-factor and as such plays a  
523 critical role in maintaining cellular homeostasis within the microorganisms [93]. Iron storage  
524 proteins, such as bacterioferritin derived from two different population genomes of  
525 *Nitrosomonas* were both downregulated after exposure to FNA (Figure S3(B)) [94]. Iron  
526 transport proteins such as haemoglobin, haemoglobin-haptoglobin binding protein and the  
527 *Nitrosomonas* ABC iron transporter as well as the catecholate siderophore receptor Flu, were  
528 all upregulated after exposure to FNA as shown in Figure S3(B) [95-98]. The haemoglobin  
529 and haemoglobin-haptoglobin-binding protein which form part of a receptor required for  
530 heme uptake is upregulated on exposure to FNA [95]. Catecholate siderophore receptor Flu  
531 are known to transport siderophore which are low molecular weight ferric ion specific  
532 chelating agents used by microorganisms to scavenge iron from the environment [99].  
533 Siderophore transport proteins were seen to be marginally upregulated on exposure to FNA  
534 as shown in Figure S3(B). As evidenced, iron transport across the membrane into the cell was  
535 facilitated signifying the change in iron levels internal of the *Nitrosomonas* genera. A  
536 decrease in expression levels of Fe-S enzymes was detected post FNA treatment (Figure  
537 S3(B)). Thus it can be clearly seen that FNA disrupts the bioavailability of cellular iron  
538 within the *Nitrosomonas* population.

539

540 The regulation of other proteins involved in key metabolic processes such as carbon  
541 dioxide fixation, respiration, TCA cycle, glycolysis, DNA replication, RNA transcription and  
542 protein translation were also studied and have been discussed in the Supplementary section



543 S6. An overview of the amino acid, fatty acid biosynthesis and breakdown and carbohydrate  
544 metabolism has also been discussed in the supplementary section S6.

545

#### 546 3.4.1.2. *Nitrobacter*

547 This study also intended to look at the response of NOB particularly *Nitrobacter*  
548 genera to the FNA. However, only 15 proteins were detected to have a  $\log_2(\text{FC})$  within the  
549 *Nitrobacter* genera (Figure S8). The low detection of *Nitrobacter* proteins by our  
550 metaproteomic approach very likely reflects the lower abundance of these microorganisms in  
551 the mixed culture community (Table S2 and S3). As such it was difficult to draw any  
552 conclusions of changes in the metabolic pathways from the limited proteins we detected. An  
553 enriched NOB culture from activated sludge would be beneficial in investigating the  
554 mechanism of NOB susceptibility to FNA.

555

#### 556 3.5. *Persistence to FNA in Nitrosomonas reveals multipronged mechanisms*

557 The tolerance of the *Nitrosomonas* can be attributed to an upregulation of oxidative  
558 stress enzymes, denitrification, DNA and protein repair mechanisms as well as other defence  
559 pathways such as the inhibition of phage formation. There was also evidence that FNA alters  
560 the cellular iron bioavailability within a cell leading to an upregulation of enzymes involved  
561 in iron transport across the membrane although the mechanism through which this occurs  
562 remains unclear. The *Nitrosomonas* population shows an upregulation of the energy  
563 producing nitrification pathway enzymes i.e. AMO and HAO despite the low ammonia and  
564 dissolved oxygen in the FNA treatment reactor. We hypothesise that this upregulation is due  
565 to a need for internal energy generation in anticipation of available ammonia. Overall  
566 *Nitrosomonas* exerts a strong response to deal with oxidative stress caused by FNA.

567

568 (Position for Figure 3)

569

570           There was strong evidence to suggest that FNA caused oxidative stress on the  
571 *Nitrosomonas* population possibly through its ROS and RNS intermediates. We developed an  
572 overview to diagrammatically represent the effects of FNA and the responses of  
573 *Nitrosomonas* to the biocide (Figure 3). This study provides a fundamental understanding of  
574 the molecular mechanisms involved in the tolerance of *Nitrosomonas* to FNA. The findings  
575 made here are relevant to applications that are based on the suppression of NOB over AOB.  
576 Use of FNA can allow for better utilisation of energy resources such in the activated sludge  
577 process and for the development of better lines of feed suited for the Anammox process.

578

579

580

581

582

583

584

585

586

587 **CORRESPONDING AUTHOR INFORMATION:**

588 **Corresponding Author**

589 \* Advanced Water Management Centre, Gehrman Laboratories Building (60), The  
590 University of Queensland, Research Rd, St Lucia QLD 4067.

591 Phone: +61 7 3346 3226: email: [phil.bond@awmc.uq.edu.au](mailto:phil.bond@awmc.uq.edu.au) (Philip.L.Bond)

592 **Notes:**

593 The authors declare no competing financial interest.

594

595

## 596 **ACKNOWLEDGEMENTS**

597 We acknowledge the Australian Research Council for funding support of project  
598 DP120102832 (Biofilm Control in Wastewater Systems using Free Nitrous Acid - a  
599 Renewable Material from Wastewater). Andrew Laloo acknowledges the Graduate School  
600 International Travel Award (GSITA), University of Queensland and the University of  
601 Queensland International Scholarship (UQI). We acknowledge the PRIDE team for the  
602 deposition of our data to the ProteomeXchange Consortium (PXD007514) and the sequence  
603 read archive for the deposition of the DNA sequencing data (SRA study: SRP115442) [45,  
604 100]. *In silico* analyses for the bioinformatic pipeline 2 were carried out using the HPC  
605 facilities of the University of Luxembourg [101]. Dr Qilin Wang acknowledges the  
606 Australian Research Council Discovery Early Career Researcher Award (DE160100667)

607

608

609

## 610 **ASSOCIATED CONTENT**

### 611 **Supplementary Information Available**

612 Supplementary data associated with this article can be found free of charge on the  
613 ACS Publication website at <http://pubs.acs.org/>.

614

615

616

617

618 **REFERENCES:**

- 619 1. Vadivelu, V.M., Yuan, Z., Fux, C., and Keller, J., The inhibitory effects of free nitrous  
620 acid on the energy generation and growth processes of an enriched nitrobacter culture.  
621 *Environ Sci Technol* **2006**, 40(14), 4442-8.
- 622 2. Zhou, Y., Ganda, L., Lim, M., Yuan, Z., Kjelleberg, S., and Ng, W.J., Free nitrous acid  
623 (FNA) inhibition on denitrifying poly-phosphate accumulating organisms (DPAOs). *Appl*  
624 *Microbiol Biotechnol* **2010**, 88(1), 359-69.
- 625 3. Pijuan, M., Ye, L., and Yuan, Z., Free nitrous acid inhibition on the aerobic metabolism of  
626 poly-phosphate accumulating organisms. *Water Res* **2010**, 44(20), 6063-72.
- 627 4. Gao, S.H., Ho, J.Y., Fan, L., Richardson, D.J., Yuan, Z., and Bond, P.L., Antimicrobial  
628 Effects of Free Nitrous Acid on *Desulfovibrio vulgaris*: Implications for Sulfide-Induced  
629 Corrosion of Concrete. *Appl Environ Microbiol* **2016**, 82(18), 5563-75.
- 630 5. Gao, S.H., Fan, L., Peng, L., Guo, J., Agullo-Barcelo, M., Yuan, Z., et al., Determining  
631 Multiple Responses of *Pseudomonas aeruginosa* PAO1 to an Antimicrobial Agent, Free  
632 Nitrous Acid. *Environ Sci Technol* **2016**, 50(10), 5305-12.
- 633 6. Wang, D., Wang, Q., Laloo, A.E., and Yuan, Z., Reducing N<sub>2</sub>O Emission from a  
634 Domestic-Strength Nitrifying Culture by Free Nitrous Acid-Based Sludge Treatment.  
635 *Environ Sci Technol* **2016**, 50(14), 7425-33.
- 636 7. Jiang, G., Gutierrez, O., and Yuan, Z., The strong biocidal effect of free nitrous acid on  
637 anaerobic sewer biofilms. *Water Res* **2011**, 45(12), 3735-43.
- 638 8. Wang, Q., Ye, L., Jiang, G., Jensen, P.D., Batstone, D.J., and Yuan, Z., Free nitrous acid  
639 (FNA)-based pretreatment enhances methane production from waste activated sludge.  
640 *Environ Sci Technol* **2013**, 47(20), 11897-904.
- 641 9. Fang, F.C., Antimicrobial reactive oxygen and nitrogen species: concepts and  
642 controversies. *Nat Rev Microbiol* **2004**, 2(10), 820-32.

- 643 10. Zhou, Y., Oehmen, A., Lim, M., Vadivelu, V., and Ng, W.J., The role of nitrite and free  
644 nitrous acid (FNA) in wastewater treatment plants. *Water Res* **2011**, 45(15), 4672-82.
- 645 11. Gao, S.H., Fan, L., Yuan, Z., and Bond, P.L., The concentration-determined and  
646 population-specific antimicrobial effects of free nitrous acid on *Pseudomonas aeruginosa*  
647 PAO1. *Appl Microbiol Biotechnol* **2015**, 99(5), 2305-12.
- 648 12. Gavrilescu, M., Demnerova, K., Aamand, J., Agathos, S., and Fava, F., Emerging  
649 pollutants in the environment: present and future challenges in biomonitoring, ecological  
650 risks and bioremediation. *N Biotechnol* **2015**, 32(1), 147-56.
- 651 13. Xie, B., Liu, B., Yi, Y., Yang, L., Liang, D., Zhu, Y., et al., Microbiological mechanism  
652 of the improved nitrogen and phosphorus removal by embedding microbial fuel cell in  
653 Anaerobic-Anoxic-Oxic wastewater treatment process. *Bioresour Technol* **2016**, 207, 109-  
654 17.
- 655 14. Henze, M., Harremoës, P., la Cour Jansen, J., and Arvin, E., *Wastewater treatment:*  
656 *biological and chemical processes*. 2001: Springer Science & Business Media.
- 657 15. Wang, D., Wang, Q., Laloo, A., Xu, Y., Bond, P.L., and Yuan, Z., Achieving Stable  
658 Nitrification for Mainstream Deammonification by Combining Free Nitrous Acid-Based  
659 Sludge Treatment and Oxygen Limitation. *Sci Rep* **2016**, 6, 25547.
- 660 16. Wang, Q., Ye, L., Jiang, G., Hu, S., and Yuan, Z., Side-stream sludge treatment using  
661 free nitrous acid selectively eliminates nitrite oxidizing bacteria and achieves the nitrite  
662 pathway. *Water Res* **2014**, 55, 245-255.
- 663 17. Kim, D.J., Seo, D.W., Lee, S.H., and Shipin, O., Free nitrous acid selectively inhibits and  
664 eliminates nitrite oxidizers from nitrifying sequencing batch reactor. *Bioprocess Biosyst*  
665 *Eng* **2012**, 35(3), 441-8.
- 666 18. Cantera, J.J. and Stein, L.Y., Molecular diversity of nitrite reductase genes (*nirK*) in  
667 nitrifying bacteria. *Environ Microbiol* **2007**, 9(3), 765-76.

- 668 19. Wei, X., Vajrala, N., Hauser, L., Sayavedra-Soto, L.A., and Arp, D.J., Iron nutrition and  
669 physiological responses to iron stress in *Nitrosomonas europaea*. *Arch Microbiol* **2006**,  
670 186(2), 107-18.
- 671 20. Gvakharia, B.O., Permina, E.A., Gelfand, M.S., Bottomley, P.J., Sayavedra-Soto, L.A.,  
672 and Arp, D.J., Global transcriptional response of *Nitrosomonas europaea* to chloroform  
673 and chloromethane. *Appl Environ Microbiol* **2007**, 73(10), 3440-5.
- 674 21. Park, S. and Ely, R.L., Genome-wide transcriptional responses of *Nitrosomonas europaea*  
675 to zinc. *Arch Microbiol* **2008**, 189(6), 541-8.
- 676 22. Wood, N.J. and Sorensen, J., Catalase and superoxide dismutase activity in ammonia-  
677 oxidising bacteria. *Fems Microbiology Ecology* **2001**, 38(1), 53-58.
- 678 23. Gillet, L.C., Navarro, P., Tate, S., Rost, H., Selevsek, N., Reiter, L., et al., Targeted data  
679 extraction of the MS/MS spectra generated by data-independent acquisition: a new  
680 concept for consistent and accurate proteome analysis. *Mol Cell Proteomics* **2012**, 11(6),  
681 O111 016717.
- 682 24. Zeng, R.J., Lemaire, R., Yuan, Z., and Keller, J., Simultaneous nitrification,  
683 denitrification, and phosphorus removal in a lab-scale sequencing batch reactor.  
684 *Biotechnol Bioeng* **2003**, 84(2), 170-8.
- 685 25. Meyer, F., Paarmann, D., D'Souza, M., Olson, R., Glass, E.M., Kubal, M., et al., The  
686 metagenomics RAST server - a public resource for the automatic phylogenetic and  
687 functional analysis of metagenomes. *BMC Bioinformatics* **2008**, 9, 386.
- 688 26. Bolger, A.M., Lohse, M., and Usadel, B., Trimmomatic: a flexible trimmer for Illumina  
689 sequence data. *Bioinformatics* **2014**, 30(15), 2114-20.
- 690 27. <https://github.com/geronimp/graftM>.
- 691 28. <https://sourceforge.net/projects/bbmap/>.

- 692 29. Imelfort, M., Parks, D., Woodcroft, B.J., Dennis, P., Hugenholtz, P., and Tyson, G.W.,  
693 GroopM: an automated tool for the recovery of population genomes from related  
694 metagenomes. *PeerJ* **2014**, 2, e603.
- 695 30. Kang, D.D., Froula, J., Egan, R., and Wang, Z., MetaBAT, an efficient tool for accurately  
696 reconstructing single genomes from complex microbial communities. *PeerJ* **2015**, 3,  
697 e1165.
- 698 31. Narayanasamy, S., Jarosz, Y., Muller, E.E., Heintz-Buschart, A., Herold, M., Kaysen, A.,  
699 et al., IMP: a pipeline for reproducible reference-independent integrated metagenomic and  
700 metatranscriptomic analyses. *Genome Biol* **2016**, 17(1), 260.
- 701 32. Laczny, C.C., Sternal, T., Plugaru, V., Gawron, P., Atashpendar, A., Margossian, H.H., et  
702 al., VizBin - an application for reference-independent visualization and human-augmented  
703 binning of metagenomic data. *Microbiome* **2015**, 3(1), 1.
- 704 33. Heintz-Buschart, A., May, P., Laczny, C.C., Lebrun, L.A., Bellora, C., Krishna, A., et al.,  
705 Integrated multi-omics of the human gut microbiome in a case study of familial type 1  
706 diabetes. *Nat Microbiol* **2016**, 2, 16180.
- 707 34. <http://gtdb.ecogenomic.org/>.
- 708 35. Parks, D.H., Imelfort, M., Skennerton, C.T., Hugenholtz, P., and Tyson, G.W., CheckM:  
709 assessing the quality of microbial genomes recovered from isolates, single cells, and  
710 metagenomes. *Genome Res* **2015**, 25(7), 1043-55.
- 711 36. Seemann, T., Prokka: rapid prokaryotic genome annotation. *Bioinformatics* **2014**, 30(14),  
712 2068-9.
- 713 37. Grobber, C., Viridis, B., Nouwens, A., Harnisch, F., Rabaey, K., and Bond, P.L., Use of  
714 SWATH mass spectrometry for quantitative proteomic investigation of *Shewanella*  
715 *oneidensis* MR-1 biofilms grown on graphite cloth electrodes. *Syst Appl Microbiol* **2015**,  
716 38(2), 135-9.

- 717 38. Kappler, U. and Nouwens, A.S., The molybdoproteome of *Starkeya novella* - insights  
718 into the diversity and functions of molybdenum containing proteins in response to  
719 changing growth conditions. *Metallomics* **2013**, 5(4), 325-334.
- 720 39. Bailey, U.M., Jamaluddin, M.F., and Schulz, B.L., Analysis of Congenital Disorder of  
721 Glycosylation-Id in a Yeast Model System Shows Diverse Site-Specific Under-  
722 glycosylation of Glycoproteins. *Journal of Proteome Research* **2012**, 11(11), 5376-5383.
- 723 40. Choi, M., Chang, C.Y., Clough, T., Broudy, D., Killeen, T., MacLean, B., et al., MSstats:  
724 an R package for statistical analysis of quantitative mass spectrometry-based proteomic  
725 experiments. *Bioinformatics* **2014**, 30(17), 2524-6.
- 726 41. The UniProt, C., UniProt: the universal protein knowledgebase. *Nucleic Acids Res* **2017**,  
727 45(D1), D158-D169.
- 728 42. Zhang, L., Zheng, P., Tang, C.J., and Jin, R.C., Anaerobic ammonium oxidation for  
729 treatment of ammonium-rich wastewaters. *J Zhejiang Univ Sci B* **2008**, 9(5), 416-26.
- 730 43. Gerardi, M.H., *Introduction to Nitrification*, in *Nitrification and Denitrification in the*  
731 *Activated Sludge Process*. 2003, John Wiley & Sons, Inc. p. 35-41.
- 732 44. Magrane, M. and UniProt, C., UniProt Knowledgebase: a hub of integrated protein data.  
733 *Database (Oxford)* **2011**, 2011, bar009.
- 734 45. Vizcaino, J.A., Cote, R.G., Csordas, A., Dianes, J.A., Fabregat, A., Foster, J.M., et al.,  
735 The Proteomics Identifications (PRIDE) database and associated tools: status in 2013.  
736 *Nucleic Acids Research* **2013**, 41(D1), D1063-D1069.
- 737 46. Bowler, C., Vanmontagu, M., and Inze, D., Superoxide-Dismutase and Stress Tolerance.  
738 *Annual Review of Plant Physiology and Plant Molecular Biology* **1992**, 43, 83-116.
- 739 47. Yu, R. and Chandran, K., Strategies of *Nitrosomonas europaea* 19718 to counter low  
740 dissolved oxygen and high nitrite concentrations. *BMC Microbiol* **2010**, 10, 70.



- 741 48. Davies, K.J., Oxidative stress: the paradox of aerobic life. *Biochem Soc Symp* **1995**, 61, 1-  
742 31.
- 743 49. Moreira, W., Leblanc, E., and Ouellette, M., The role of reduced pterins in resistance to  
744 reactive oxygen and nitrogen intermediates in the protozoan parasite *Leishmania*. *Free*  
745 *Radic Biol Med* **2009**, 46(3), 367-75.
- 746 50. Lu, S.C., S-Adenosylmethionine. *Int J Biochem Cell Biol* **2000**, 32(4), 391-5.
- 747 51. Cavallaro, R.A., Fusco, A., Nicolia, V., and Scarpa, S., S-adenosylmethionine prevents  
748 oxidative stress and modulates glutathione metabolism in TgCRND8 mice fed a B-vitamin  
749 deficient diet. *J Alzheimers Dis* **2010**, 20(4), 997-1002.
- 750 52. Karaa, A., Thompson, K.J., McKillop, I.H., Clemens, M.G., and Schrum, L.W., S-  
751 adenosyl-L-methionine attenuates oxidative stress and hepatic stellate cell activation in an  
752 ethanol-LPS-induced fibrotic rat model. *Shock* **2008**, 30(2), 197-205.
- 753 53. Foote, N., Thompson, A.C., Barber, D., and Greenwood, C., Pseudomonas cytochrome  
754 C-551 peroxidase. A purification procedure and study of CO-binding kinetics. *Biochem J*  
755 **1983**, 209(3), 701-7.
- 756 54. Korshunov, S.S., Krasnikov, B.F., Pereverzev, M.O., and Skulachev, V.P., The  
757 antioxidant functions of cytochrome c. *FEBS Lett* **1999**, 462(1-2), 192-8.
- 758 55. Campos, E.G., Hermes-Lima, M., Smith, J.M., and Prichard, R.K., Characterisation of  
759 *Fasciola hepatica* cytochrome c peroxidase as an enzyme with potential antioxidant  
760 activity in vitro. *International Journal for Parasitology* **1999**, 29(5), 655-662.
- 761 56. Powis, G. and Montfort, W.R., Properties and biological activities of thioredoxins. *Annu*  
762 *Rev Biophys Biomol Struct* **2001**, 30, 421-55.
- 763 57. Vieira Dos Santos, C. and Rey, P., Plant thioredoxins are key actors in the oxidative  
764 stress response. *Trends Plant Sci* **2006**, 11(7), 329-34.

- 765 58. Fernando, M.R., Nanri, H., Yoshitake, S., Nagata-Kuno, K., and Minakami, S.,  
766 Thioredoxin regenerates proteins inactivated by oxidative stress in endothelial cells. *Eur J*  
767 *Biochem* **1992**, 209(3), 917-22.
- 768 59. Saleh, M., Bartual, S.G., Abdullah, M.R., Jensch, I., Asmat, T.M., Petruschka, L., et al.,  
769 Molecular architecture of *Streptococcus pneumoniae* surface thioredoxin-fold lipoproteins  
770 crucial for extracellular oxidative stress resistance and maintenance of virulence. *EMBO*  
771 *Mol Med* **2013**, 5(12), 1852-70.
- 772 60. Xia, L., Bjornstedt, M., Nordman, T., Eriksson, L.C., and Olsson, J.M., Reduction of  
773 ubiquinone by lipoamide dehydrogenase. An antioxidant regenerating pathway. *Eur J*  
774 *Biochem* **2001**, 268(5), 1486-90.
- 775 61. Lowther, W.T., Brot, N., Weissbach, H., and Matthews, B.W., Structure and mechanism  
776 of peptide methionine sulfoxide reductase, an "anti-oxidation" enzyme. *Biochemistry*  
777 **2000**, 39(44), 13307-12.
- 778 62. Weissbach, H., Etienne, F., Hoshi, T., Heinemann, S.H., Lowther, W.T., Matthews, B., et  
779 al., Peptide methionine sulfoxide reductase: structure, mechanism of action, and biological  
780 function. *Arch Biochem Biophys* **2002**, 397(2), 172-8.
- 781 63. Broxton, C.N. and Culotta, V.C., SOD Enzymes and Microbial Pathogens: Surviving the  
782 Oxidative Storm of Infection. *PLoS Pathog* **2016**, 12(1), e1005295.
- 783 64. Cabiscol, E., Tamarit, J., and Ros, J., Oxidative stress in bacteria and protein damage by  
784 reactive oxygen species. *Int Microbiol* **2000**, 3(1), 3-8.
- 785 65. Poth, M. and Focht, D.D., N Kinetic Analysis of N(2)O Production by *Nitrosomonas*  
786 *europaea*: an Examination of Nitrifier Denitrification. *Appl Environ Microbiol* **1985**,  
787 49(5), 1134-41.
- 788 66. Arp, D.J. and Stein, L.Y., Metabolism of inorganic N compounds by ammonia-oxidizing  
789 bacteria. *Crit Rev Biochem Mol Biol* **2003**, 38(6), 471-95.

- 790 67. Beaumont, H.J., Hommes, N.G., Sayavedra-Soto, L.A., Arp, D.J., Arciero, D.M., Hooper,  
791 A.B., et al., Nitrite reductase of *Nitrosomonas europaea* is not essential for production of  
792 gaseous nitrogen oxides and confers tolerance to nitrite. *J Bacteriol* **2002**, 184(9), 2557-  
793 60.
- 794 68. Cabello, P., Pino, C., Olmo-Mira, M.F., Castillo, F., Roldan, M.D., and Moreno-Vivian,  
795 C., Hydroxylamine assimilation by *Rhodobacter capsulatus* E1F1. requirement of the hep  
796 gene (hybrid cluster protein) located in the nitrate assimilation nas gene region for  
797 hydroxylamine reduction. *J Biol Chem* **2004**, 279(44), 45485-94.
- 798 69. Wilhelm, R., Abeliovich, A., and Nejidat, A., Effect of long-term ammonia starvation on  
799 the oxidation of ammonia and hydroxylamine by *Nitrosomonas europaea*. *J Biochem*  
800 **1998**, 124(4), 811-5.
- 801 70. Stein, L.Y. and Arp, D.J., Loss of ammonia monooxygenase activity in *Nitrosomonas*  
802 *europaea* upon exposure to nitrite. *Applied and Environmental Microbiology* **1998**, 64(10),  
803 4098-4102.
- 804 71. Weber, J., Structural biology: Toward the ATP synthase mechanism. *Nat Chem Biol*  
805 **2010**, 6(11), 794-5.
- 806 72. Gao, S.H., Ho, J.Y., Fan, L., Richardson, D.J., Yuan, Z., and Bond, P.L., Antimicrobial  
807 effects of free nitrous acid on *Desulfovibrio vulgaris*: implications for sulfide induced  
808 concrete corrosion. *Appl Environ Microbiol* **2016**.
- 809 73. Meyer, R.R. and Laine, P.S., The single-stranded DNA-binding protein of *Escherichia*  
810 *coli*. *Microbiol Rev* **1990**, 54(4), 342-80.
- 811 74. Grove, A., Functional evolution of bacterial histone-like HU proteins. *Curr Issues Mol*  
812 *Biol* **2011**, 13(1), 1-12.
- 813 75. Bernstein, K.A., Gangloff, S., and Rothstein, R., The RecQ DNA helicases in DNA  
814 repair. *Annu Rev Genet* **2010**, 44, 393-417.

- 815 76. Tsai, W. and Clarke, S., Amino acid polymorphisms of the human L-isopartyl/D-  
816 aspartyl methyltransferase involved in protein repair. *Biochem Biophys Res Commun*  
817 **1994**, 203(1), 491-7.
- 818 77. Clarke, S., A protein carboxyl methyltransferase that recognizes age-damaged peptides  
819 and proteins and participates in their repair. *S-adenosylmethionine-dependent*  
820 *methyltransferases: structures and functions*. *World Scientific, Singapore* **1999**, 123-148.
- 821 78. St John, G., Brot, N., Ruan, J., Erdjument-Bromage, H., Tempst, P., Weissbach, H., et al.,  
822 Peptide methionine sulfoxide reductase from *Escherichia coli* and *Mycobacterium*  
823 *tuberculosis* protects bacteria against oxidative damage from reactive nitrogen  
824 intermediates. *Proc Natl Acad Sci U S A* **2001**, 98(17), 9901-6.
- 825 79. Lee, S., Sowa, M.E., Watanabe, Y.H., Sigler, P.B., Chiu, W., Yoshida, M., et al., The  
826 structure of clpB: A molecular chaperone that rescues proteins from an aggregated state.  
827 *Cell* **2003**, 115(2), 229-240.
- 828 80. Gvakharia, B.O., Bottomley, P.J., Arp, D.J., and Sayavedra-Soto, L.A., Construction of  
829 recombinant *Nitrosomonas europaea* expressing green fluorescent protein in response to  
830 co-oxidation of chloroform. *Appl Microbiol Biotechnol* **2009**, 82(6), 1179-85.
- 831 81. Dubaquié, Y., Looser, R., and Rospert, S., Significance of chaperonin 10-mediated  
832 inhibition of ATP hydrolysis by chaperonin 60. *Proc Natl Acad Sci U S A* **1997**, 94(17),  
833 9011-6.
- 834 82. Dy, R.L., Przybilski, R., Semeijn, K., Salmond, G.P., and Fineran, P.C., A widespread  
835 bacteriophage abortive infection system functions through a Type IV toxin-antitoxin  
836 mechanism. *Nucleic Acids Res* **2014**, 42(7), 4590-605.
- 837 83. Barraud, N., Schleheck, D., Klebensberger, J., Webb, J.S., Hassett, D.J., Rice, S.A., et al.,  
838 Nitric Oxide Signaling in *Pseudomonas aeruginosa* Biofilms Mediates Phosphodiesterase

- 839 Activity, Decreased Cyclic Di-GMP Levels, and Enhanced Dispersal. *Journal of*  
840 *Bacteriology* **2009**, 191(23), 7333-7342.
- 841 84. Kihara, A., Akiyama, Y., and Ito, K., A protease complex in the Escherichia coli plasma  
842 membrane: HflKC (HflA) forms a complex with FtsH (HflB), regulating its proteolytic  
843 activity against SecY. *EMBO J* **1996**, 15(22), 6122-31.
- 844 85. Dortet, L., Girlich, D., Virlouvet, A.L., Poirel, L., Nordmann, P., Iorga, B.I., et al.,  
845 Characterization of BRPMBL, the Bleomycin Resistance Protein Associated with the  
846 Carbapenemase NDM. *Antimicrob Agents Chemother* **2017**, 61(3), e02413-16.
- 847 86. Chen, J. and Stubbe, J., Bleomycins: towards better therapeutics. *Nat Rev Cancer* **2005**,  
848 5(2), 102-12.
- 849 87. Petrovich, M., Wu, C.-Y., Rosenthal, A., Chen, K.-F., Packman, A.I., and Wells, G.F.,  
850 Nitrosomonas europaea biofilm formation is enhanced by Pseudomonas aeruginosa.  
851 *FEMS Microbiology Ecology* **2017**, 93(5), fix047.
- 852 88. Schmidt, I., Steenbakkens, P.J., op den Camp, H.J., Schmidt, K., and Jetten, M.S.,  
853 Physiologic and proteomic evidence for a role of nitric oxide in biofilm formation by  
854 Nitrosomonas europaea and other ammonia oxidizers. *J Bacteriol* **2004**, 186(9), 2781-8.
- 855 89. Boyd, A. and Chakrabarty, A.M., Pseudomonas aeruginosa biofilms: role of the alginate  
856 exopolysaccharide. *J Ind Microbiol* **1995**, 15(3), 162-8.
- 857 90. Barbosa, R.L. and Benedetti, C.E., BigR, a transcriptional repressor from plant-associated  
858 bacteria, regulates an operon implicated in biofilm growth. *J Bacteriol* **2007**, 189(17),  
859 6185-94.
- 860 91. Olvera, C., Goldberg, J.B., Sanchez, R., and Soberon-Chavez, G., The Pseudomonas  
861 aeruginosa algC gene product participates in rhamnolipid biosynthesis. *Fems*  
862 *Microbiology Letters* **1999**, 179(1), 85-90.

- 863 92. Sakoh, M., Ito, K., and Akiyama, Y., Proteolytic activity of HtpX, a membrane-bound  
864 and stress-controlled protease from Escherichia coli. *J Biol Chem* **2005**, 280(39), 33305-  
865 10.
- 866 93. Payne, S.M. and Finkelstein, R.A., The critical role of iron in host-bacterial interactions. *J*  
867 *Clin Invest* **1978**, 61(6), 1428-40.
- 868 94. Rivera, M., Bacterioferritin: Structure, Dynamics, and Protein-Protein Interactions at Play  
869 in Iron Storage and Mobilization. *Accounts of Chemical Research* **2017**, 50(2), 331-340.
- 870 95. Seale, T.W., Morton, D.J., Whitby, P.W., Wolf, R., Kosanke, S.D., VanWagoner, T.M.,  
871 et al., Complex role of hemoglobin and hemoglobin-haptoglobin binding proteins in  
872 Haemophilus influenzae virulence in the infant rat model of invasive infection. *Infect*  
873 *Immun* **2006**, 74(11), 6213-25.
- 874 96. Koster, W., ABC transporter-mediated uptake of iron, siderophores, heme and vitamin  
875 B12. *Res Microbiol* **2001**, 152(3-4), 291-301.
- 876 97. Saha, M., Sarkar, S., Sarkar, B., Sharma, B.K., Bhattacharjee, S., and Tribedi, P.,  
877 Microbial siderophores and their potential applications: a review. *Environ Sci Pollut Res*  
878 *Int* **2016**, 23(5), 3984-99.
- 879 98. Vajrala, N., Sayavedra-Soto, L.A., Bottomley, P.J., and Arp, D.J., Role of Nitrosomonas  
880 europaea NitABC iron transporter in the uptake of Fe<sup>3+</sup>-siderophore complexes. *Arch*  
881 *Microbiol* **2010**, 192(11), 899-908.
- 882 99. Neilands, J.B., Siderophores: structure and function of microbial iron transport  
883 compounds. *J Biol Chem* **1995**, 270(45), 26723-6.
- 884 100. Leinonen, R., Sugawara, H., Shumway, M., and International Nucleotide Sequence  
885 Database, C., The sequence read archive. *Nucleic Acids Res* **2011**, 39(Database issue),  
886 D19-21.

887 101. Varrette, S., Bouvry, P., Cartiaux, H., and Georgatos, F. *Management of an academic*  
888 *HPC cluster: The UL experience.* in *2014 International Conference on High Performance*  
889 *Computing & Simulation (HPCS)*. 2014.

890

891

892

893

894

895

896

897

898

899

900

901

902

903

904

905

906

907

908

909

910 Table 1: The population genome bins from metagenomic pipeline 1 and 2, of known nitrifiers  
 911 generated from the reactor and the publically available genomes that were combined and  
 912 added to the custom database for metaproteomic analyses.

	Genomes	Code names	Completeness (%)	Contamination	Average fold coverage (X)	Scaffolds with coverage (%)	Bin bases covered (%)
Metagenome Population genome bins	<b><i>Nitrosomonas</i> genus</b>						
	Pipeline 1						
	<i>Nitrosomonas_99</i>	Ns99	99.52	1.46	3051.57	100	99.96
	<i>Nitrosomonas_89</i>	Ns89	89.13	2.45	1164.01	100	100
	<i>Nitrosomonas_82</i>	Ns82	82.31	4.23	165.11	100	99.99
	Pipeline 2						
	<i>Nitrosomonas_01321</i>	Ns85	85.2	9.78	1233.78	100	100
	<i>Nitrosomonas_L1322</i>	Ns79	76.52	1.13	3057.37	100	100
	<b><i>Nitrobacter</i> genus</b>						
	Pipeline 1						
	<i>Nitrobacter_95</i>	Nb95	95.99	1.42	219.73	100	100
	<i>Nitrobacter_88</i>	Nb88	88.88	1.69	221.64	100	99.98
	<i>Nitrobacter_79</i>	Nb79	79.96	2.38	116.9	100	99.97
	Pipeline 2						
<i>Nitrobacter_G121121</i>	Nb83	83.33	7.71	212.39	100	100	
Publically available nitrifier genomes (NCBI)	<b><i>Nitrosomonas</i> genus</b>						
	<i>Nitrosomonas Ureae</i>	NsU					
	<i>Nitrosomonas sp AL212</i>	NsA					
	<i>Nitrosomonas Eutropha C91</i>	NsEt					
	<i>Nitrosomonas Europaea</i>	NsEr					
	<i>Nitrosomonas Cryotolerans</i>	NsCr					
	<i>Nitrosomonas Communis</i>	NsC					
	<b><i>Nitrobacter</i> genus</b>						
	<i>Nitrobacter Winogradskyi</i>	NbW					
	<i>Nitrobacter Hamburgensis</i>	NbH					
<i>Nitrobacter sp Nb-311A</i>	NbN						

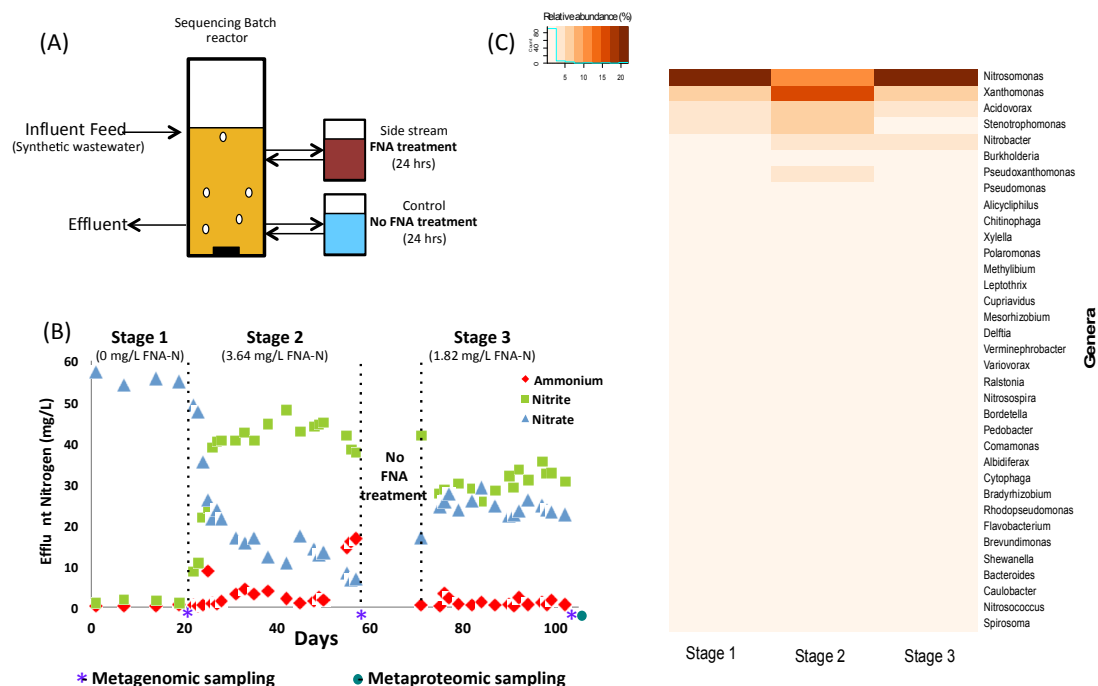
913

914

915

916





917

918 Figure 1. (A) A schematic representation of the configuration of the SBR reactor and the side  
 919 stream reactor wherein FNA treatment was carried out. (B) Levels of ammonium, nitrate and  
 920 nitrite detected in the effluent of the SBR reactor at the 3 different operational stages (Stages  
 921 1, 2, and 3) (C) The microbial community compositions of the SBR reactor during the 3  
 922 operational stages showing the dominant *Nitrosomonas* genus as derived from MG-RAST.

923

924

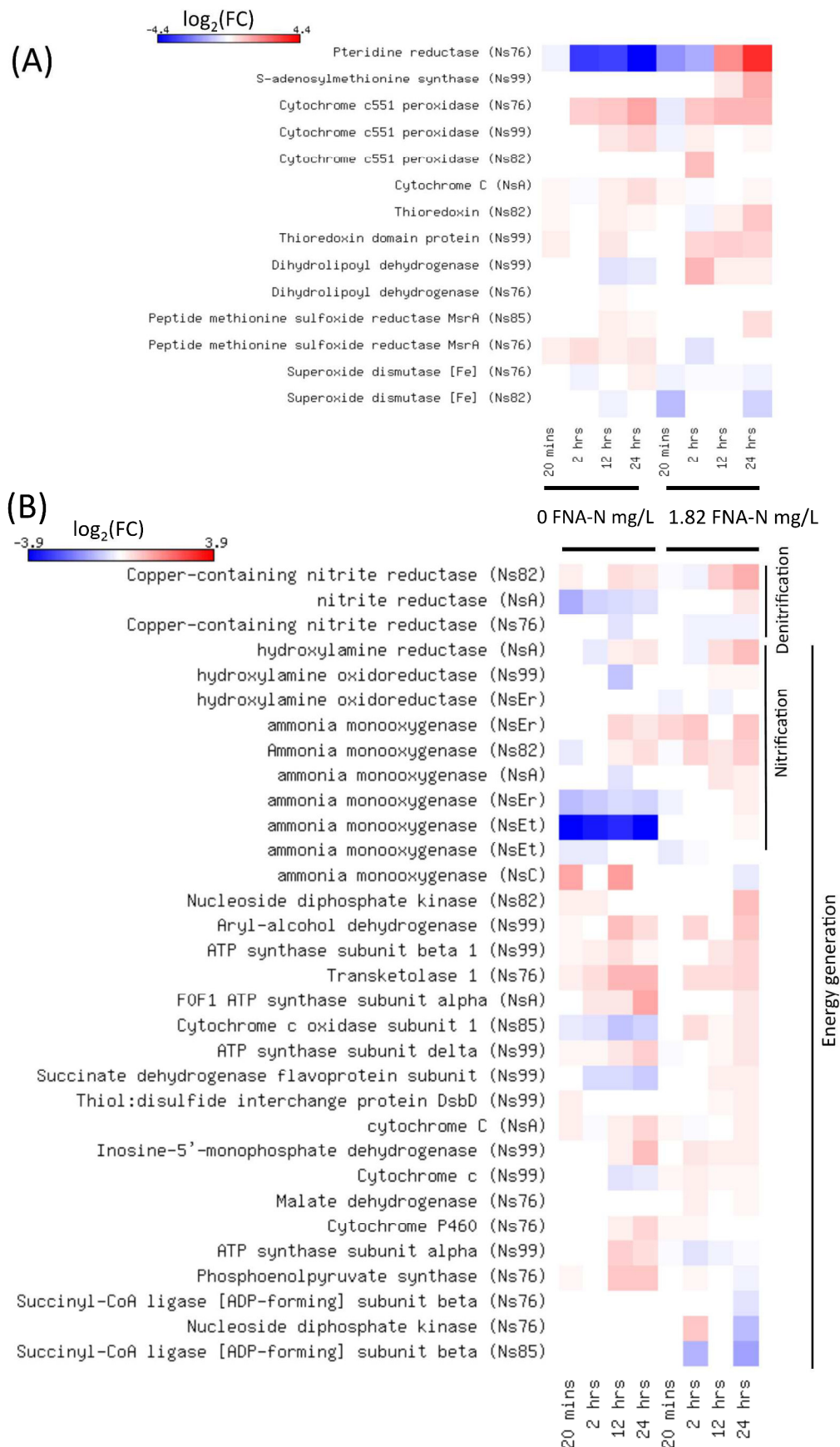
925

926

927

928

929



930 Figure 2: Heatmap showing the regulation of (A) Oxidative stress proteins and (B) enzymes

931 involved in the nitrogen metabolism and energy generation represented as  $\log_2(\text{FC})$  across  
932 both the 0 and 1.82 mg/L FNA-N conditions. The names within the brackets indicate the  
933 population genomes from where the respective genes were derived as shown in Table 1.  
934 White sections within the heatmap represent data wherein triplicates did not meet the  
935 stringency levels of p-value  $p \leq 0.05$ . Blue represent a negative  $\log_2(\text{FC})$  and red represents a  
936 positive  $\log_2(\text{FC})$ .

937

938

939

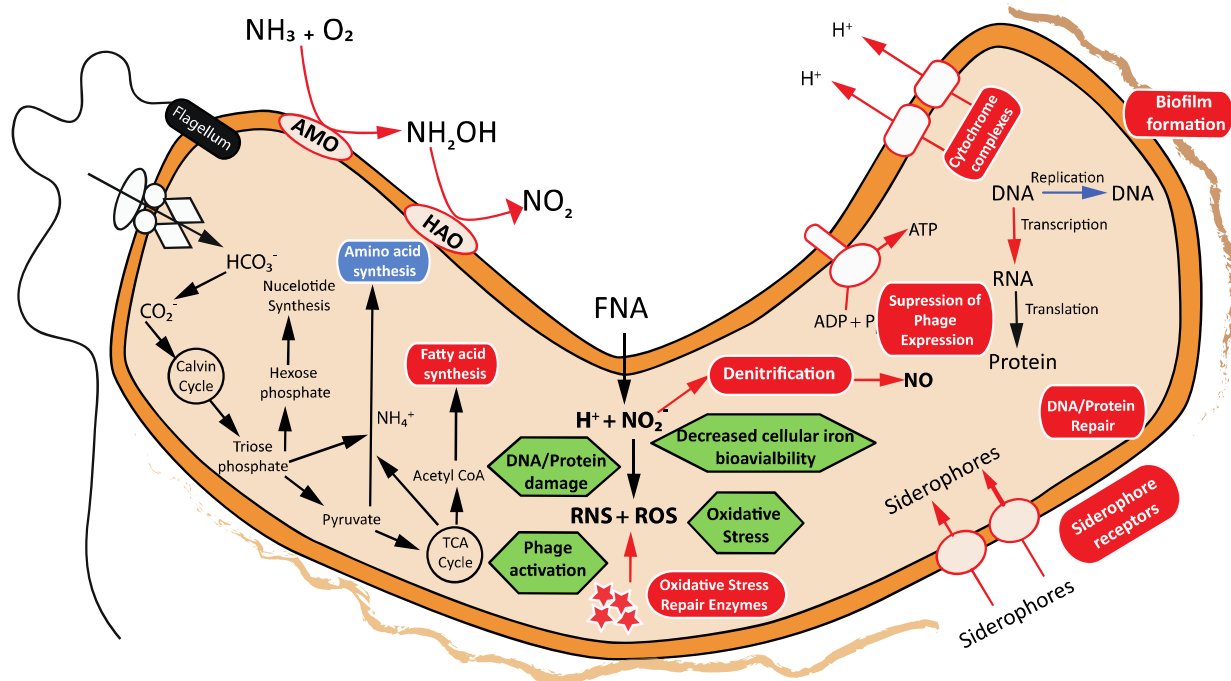
940

941

942

943

944



945 Figure 3: An overview model of the responses of *Nitrosomonas* on exposure to FNA. The red  
 946 arrows and boxes (■) represent metabolic pathways that are upregulated, the blue arrows  
 947 and boxes (■) represent metabolic pathways that are downregulated and the green boxes (■)  
 948 indicate the main mechanisms of biocide action of FNA within the *Nitrosomonas* genus.

949